Histone H2A variants confer specific properties to nucleosomes and impact on chromatin accessibility

Akihisa Osakabe[1],[†], Zdravko J. Lorković[1],[†], Wataru Kobayashi[2], Hiroaki Tachiwana[2], Ramesh Yelagandula[1], Hitoshi Kurumizaka[2] and Frédéric Berger[1],*

[1]Gregor Mendel Institute (GMI), Austrian Academy of Sciences, Vienna BioCenter (VBC), Dr. Bohr-Gasse 3, 1030 Vienna, Austria and [2]Graduate School of Advanced Science and Engineering, Waseda University, 2-2 Wakamatsu-cho, Shinjuku-ku, Tokyo 162-8480, Japan

ABSTRACT

In eukaryotes, variants of core histone H2A are selectively incorporated in distinct functional domains of chromatin and are distinguished by conserved sequences of their C-terminal tail, the L1 loop and the docking domain, suggesting that each variant confers specific properties to the nucleosome. Chromatin of flowering plants contains four types of H2A variants, which biochemical properties have not been characterized. We report that in contrast with animals, in *Arabidopsis thaliana* H2A variants define only four major types of homotypic nucleosomes containing exclusively H2A, H2A.Z, H2A.X or H2A.W. *In vitro* assays show that the L1 loop and the docking domain confer distinct stability of the nucleosome. *In vivo* and *in vitro* assays suggest that the L1 loop and the docking domain cooperate with the C-terminal tail to regulate chromatin accessibility. Based on these findings we conclude that the type of H2A variant in the nucleosome impacts on its interaction with DNA and propose that H2A variants regulate the dynamics of chromatin accessibility. In plants, the predominance of homotypic nucleosomes with specific physical properties and their specific localization to distinct domains suggest that H2A variants play a dominant role in chromatin dynamics and function.

INTRODUCTION

Histone variants are functionally-defined isoforms of core histones and are found primarily in families of histones H3 and H2A ([1–3]). While a very limited set of histone variants exist in unicellular eukaryotes, a progressive expansion in the diversity and number of genes coding for histone variants is observed in multicellular species of all taxa, with a particularly sharp increase among vertebrates and land plants ([2,4]). Although most histone variants evolved independently, many acquired similar functions in land plants and animals. Such a degree of functional evolutionary convergence indicates that histone variants confer important functions ([2,5–7]). This idea is supported by structural data showing that histone variants alter nucleosome properties ([3,8–18]). Some histone variants evolved only amongst specific taxa, such as testicular H3 in mammals ([19,20]), sperm specific variants in plants ([21]), H2A.W in land plants ([22]), macroH2A in metazoans ([23]), H2A.L and H2A.B in mammals ([24]) and sperm specific variants H2A.Q and H2A.R in mammals ([25]).

The variants from the H2A family are distinguished primarily by motifs in their C-terminal tail ([2,4,7,26]). In land plants, amongst H2A variants, H2A.W contains the longest C-terminal tail with the motif KSPKK and is associated with constitutive heterochromatin ([22]). In contrast H2A.Z and H2A are primarily associated with euchromatin and decorate gene bodies ([22]). H2A.X is characterized by the SQEF/Y motif in the C-terminal tail, which is phosphorylated in response to DNA damage in *Arabidopsis* ([5,27,28]) as in other eukaryotes ([29]). In addition to the distinctive sequences of C-terminal tails, two other regions differentiate the four H2A variants. The L1 loop connects the two H2A variants in the nucleosome and the docking domain placed at the DNA entry/exit site is implicated in interactions with the $(H3–H4)_2$-tetramer within the nucleosome ([4,30,31]). The *Arabidopsis* genome contains 12 genes encoding four isoforms of canonical H2A, two isoforms of H2A.X, three isoforms of H2A.Z and three isoforms of H2A.W ([22]). Among the three *H2A.W* genes, H2A.W.6 and H2A.W.7 are expressed predominantly in vegetative tissues. They are distinguished from each other by the presence of the SQAE motif in the C-terminal tail of H2A.W.7, which

plays a role in response to DNA damage in heterochromatin (5).

Here, we establish that in *Arabidopsis* chromatin, nucleosomes contain only a single type of H2A variant, either H2A, H2A.Z, H2A.X or H2A.W, suggesting a strong impact of H2A variants on the properties of nucleosomes. We show that the L1 and docking domains confer distinct stability to nucleosomes and impact on chromatin accessibility *in vitro* and *in vivo*. Furthermore, the C-terminal tail of H2A.W interacts with the linker DNA, suggesting the specific role in a higher order chromatin structure.

MATERIALS AND METHODS

Nuclei isolation, preparation of MNase nuclear extracts and immunoprecipitation of nucleosomes

For nuclei isolation followed by MNase digestion and immunoprecipitation four grams of 3 weeks old leaves were used. Nuclei isolation, MNase digestion and immunoprecipitations were as described in (5). After immunoprecipitation the beads were resuspended in 100 μl of 0.3× PBS, mixed with 30 μl of 5× loading buffer and 15 μl were loaded per lane (for variant-specific blots) or 10 μl for H3 blots. Nuclear protein extracts for western blot analyses (Supplementary Figure S3) were prepared from 250 mg of tissue (2–3 weeks old leaves or 10–12 days old seedlings) as described in (5).

Generation of transgenic plants expressing H2A.W.6 mutants

Mutations in H2A.W.6 were introduced by gene synthesis (Invitrogene, GeneArt). Constructs expressing mutants under the control of the H2A.W.6 promoter (∼1200 bp upstream of the ATG) fused to HA tag were inserted into pCBK02 binary vector. Plants heterozygous for *h2a.w.7* and homozygous for *h2a.w.6* were transformed by floral dip method (32) and T1 transgenic plants were selected on MS plates containing 10 μg/ml phosphinothricin. T1 transgenics were analyzed by western blotting and only plants homozygous for both *h2a.w.6* and *h2a.w.7* were selected. T2 transgenic plants segregating 3:1 for the selection marker were kept and T3 generations which did not segregate for the selection marker (homozygous) were selected for further analysis.

MNase digestion profiles

Nuclei from transgenic plants expressing H2A.W.6 mutants were isolated by NIB method (5), washed once in 10 ml of N buffer (15 mM Tris–HCl pH 7.5, 60 mM KCl, 15 mM NaCl, 5 mM MgCl$_2$, 1 mM CaCl$_2$, 250 mM sucrose, 1 mM DTT, 10 mM ß-glycerophosphate) and protease inhibitors (Roche), once in one ml of N buffer and finally resuspended in 1 ml of N buffer (total volume). Ten microliters of MNase (0.01 u/μl) were added and 200 μl aliquots were taken at 0, 5, 10 and 15 min. DNA was phenol/chloroform extracted and precipitated with ethanol with addition of 2 μg of glycogen. DNA was analyzed by native 2% agarose PAGE. The gel images of digested DNA were acquired by ImageDoc (BioRad) and quantified by using ImageJ software.

Immunostaining and microscopy

Nuclei isolated from 2 to 3 weeks old leaves were processed for immunostaining as described earlier (22). H2A.W.6 antibody was used at a 1:200 dilution. Secondary antibody was Alexa 488 goat anti-rabbit at 1:500 dilution. Nuclei were counterstained with DAPI to visualize the DNA. Images were acquired with a Zeiss laser scanning confocal microscope and further processed in Photoshop for publication.

Cloning, expression, and purification of recombinant *Arabidopsis* histones

The DNA fragment encoding *Arabidopsis thaliana* H2A.13, H2A.W.6, H2A.X.3, H2B, H3.1, H4 and H2A.W.6 swap mutants were inserted into the pET15b vector (Novagen). H2A.Z.9 DNA fragment was inserted into the pET28a vector (Novagen). The recombinant histones except for H4 were expressed in *Esherichia coli* BL21 (DE3). The recombinant H4 was expressed with *E. coli* Rosetta-gami B pLysS or *E. coli* JM109 (DE3) which contain the minor tRNA expression vector (Codon (+) RIL, Stratagene). Purification of *Arabidopsis thaliana* histones was performed by the method described previously (33,34). The truncation mutants and swapping mutants of H2A.W.6 were also purified as the same methods.

Preparation of nucleosomes

The histone octamer was reconstituted as described previously (33). The nucleosome was reconstituted with purified histone octamer and the 193 base-pair (35) DNA fragment containing Widom 601 sequence (36) by the salt dialysis method, as described previously (33). The reconstituted nucleosomes were further purified by polyacrylamide gel electrophoresis, using Prep Cell apparatus (Bio-Rad).

Thermal stability assay

The thermal stability assay was performed as described previously (37). The nucleosome containing the 193 base-pair Widom 601 DNA was mixed with 5× SYPRO Orange, in 18 mM Tris–HCl (pH7.5) buffer containing 100 mM NaCl and 0.9 mM DTT. The fluorescence signals of the SYPRO Orange were detected with a StepOnePlus Real-Time PCR unit (Applied Biosystems), with a temperature gradient from 26 to 95°C, in steps of 1°C/min. The fluorescence intensity was normalized as follows: $[F(T) - F(26°C)/[F(95°C) - F(26°C)]$. $F(T)$ indicates the fluorescence intensity at a particular temperature. Or the fluorescence signal of the SYPRO Orange was detected with a LightCycler 96 (Roche), with a temperature gradient from 37 to 95°C, in steps of 0.04°C/s. The fluorescence intensity was normalized as follows: $[F(T) - F(50°C)/[F(95°C) - F(50°C)]$. $F(T)$ indicates the fluorescence intensity as a particular temperature.

MNase treatment assay

Nucleosomes (1.2 μg) were incubated at 25°C for 1, 3, 6, 9 and 15 min, in the presence of 0.006 u of MNase

(NEB). This assay was performed in 60 μl of reaction solution, containing 30 mM Tris–HCl (pH7.5), 5 mM NaCl, 2.5 mM CaCl$_2$ and 1.5 mM DTT. After incubation, 10 μl of each aliquot was mixed with deproteinization solution, containing 20 mM Tris–HCl (pH7.5), 80 mM EDTA, 80 mM EGTA, 0.25% SDS and 0.5 mg/ml proteinase K, to stop the reaction. Resulting DNA was extracted by phenol-chloroform and then analyzed by non-denaturing 10% polyacrylamide gel electrophoresis in 0.5× TBE (45 mM Tris, 45 mM boric acid and 1.6 mM EDTA). The gel was stained with ethidium bromide and DNA was visualized by ImageDoc (BioRad). The quantification was performed by using ImageJ software or Image Lab software (BioRad).

SDS-PAGE and western blotting

Proteins were resolved on 15% SDS-PAGE and stained with Coomassie blue or are transferred to nitrocellulose membrane (Protran, GE Healthcare). Western blotting was performed according to standard procedure with antibodies against *Arabidopsis* histone variants (5,22) diluted at 1 μg/ml. The H3 specific antibody (Abcam 1791) was used at 1:5000 dilution. Rat anti-HA antibody (Roche 3F10) was used at 1:2000 dilution. Secondary antibodies were goat anti-rabbit IgG (BioRad) and goat-anti rat IgG (Sigma) at 1:10 000 dilution. Blots were developed with enhanced chemiluminiscence kit (Thermo Fisher Scientific) and signals were recorded by using ChemiDoc instrument (BioRad). Signal quantifications were done with ChemiDoc software by using volume tool.

RESULTS

Arabidopsis nucleosomes are homotypic relative to their composition in H2A variants

Heterotypic nucleosomes containing two different H2A variants were reported in *Drosophila*, mouse, human, and budding yeast (38–40). In plants, the composition of nucleosomes *in vivo* and biochemical properties of nucleosomes have not been addressed systematically. In *Arabidopsis* we reported that H2A.X exists primarily in nucleosomes which are devoid of H2A.W and H2A.Z, suggesting that H2A.X nucleosomes are homotypic (5). Furthermore, the marked preferential occupancy of distinct genomic domains for each type of *Arabidopsis* H2A variant (22) also suggested that most nucleosomes contain a single type of H2A variant and are therefore homotypic. To test this hypothesis further we obtained mononucleosomes from MNase digested chromatin and analyzed their composition by immunoprecipitation using specific antibodies against each type of H2A variant (Figure 1). Overall, the very large majority of nucleosomes contained a single type of variant (Figure 1B). Only trace amounts of H2A and H2A.X were detected in H2A.W immunoprecipitations, which could be attributed to small proportion of dinucleosomes in our chromatin preparations (Figure 1A). Co-precipitation of H2A.W.6 and H2A.W.7 (Figure 1B) (5) suggests that heterotypic nucleosome containing isoforms from the same variant family could be formed, although there was a striking predominance of homotypic nucleosomes containing either only H2A.W.6 or
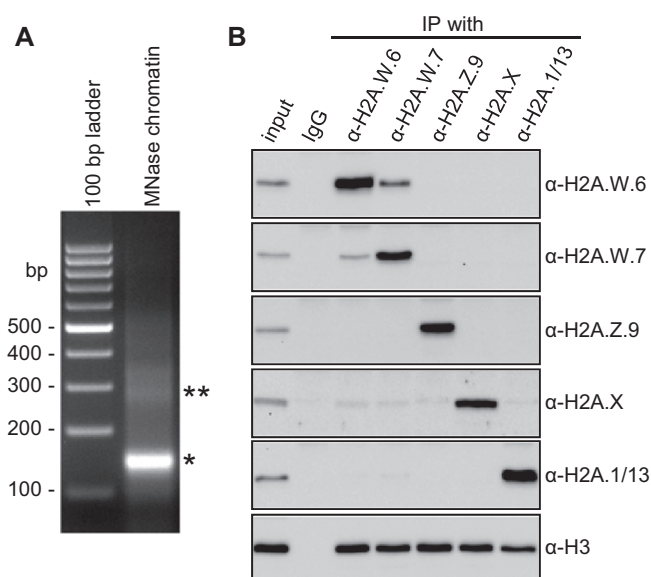

Figure 1. *Arabidopsis* H2A nucleosome are homotypic. (**A**) DNA isolated from MNase digested nuclei demonstrating almost complete digestion of chromatin into mononucleosomes (*). Small proportion of chromatin was digested into dinucleosomes (**). (**B**) Extracts from MNase digested nuclei were immunoprecipitated with antibodies against H2A.W.6, H2A.W.7, H2A.1/13, H2A.X and H2A.Z.9 histone H2A variants and analyzed by western blotting with indicated antibodies. Detection of H3 is used as a control for nucleosome integrity. In this particular experiment we observed that H2A.W.6 nucleosomes contained 19% of heterotypic nucleosomes with H2A.W.7 and H2A.W.7 nucleosomes contained 15% of heterotypic nucleosomes with H2A.W.6. (Note that antibody against the canonical H2A recognizes two variants H2A.1 and H2A.13 (22).)

H2A.W.7 (on average 19% of H2A.W nucleosomes are heterotypic for both isoforms). We thus conclude that *Arabidopsis* nucleosomes are primarily homotypic relative to their content in H2A variants, suggesting that H2A variants confer specific properties to nucleosomes.

H2A variants confer distinct stability to the nucleosome

In *Arabidopsis* each class of H2A variant comprises two to four very similar proteins (2,4). We showed previously that the combination of three features, the amino acid sequence of the C-terminal tail (CT), the L1 loop and the docking domain, define unambiguously each class of H2A variants in flowering plants (4) (Figure 2). Thus, to represent each class in further experiments, we used H2A.Z.9, H2A.X.3, H2A.W.6 and H2A.13 that are the most abundantly expressed in vegetative tissues (22) and hereafter we will refer simply to H2A.Z, H2A.X, H2A.W and H2A, unless stated otherwise. To compare biochemical properties of homotypic nucleosomes containing H2A, H2A.X, H2A.W and H2A.Z, we reconstituted nucleosomes *in vitro* by salt dialysis method (Figure 3A and B and Supplementary Figure S1B). The stability of nucleosomes was assessed by the thermal stability assay with the fluorescent dye SYPRO Orange. In this assay fluorescence is detected only when SYPRO orange binds to histones dissociated from nucleosomes (Figure 3C) (37). H2A.Z-H2B dimers dissociated from the nucleosome at much lower temperature than H2A–H2B and H2A.W–H2B (Figure 3D) or H2A.X (Supplementary Fig-
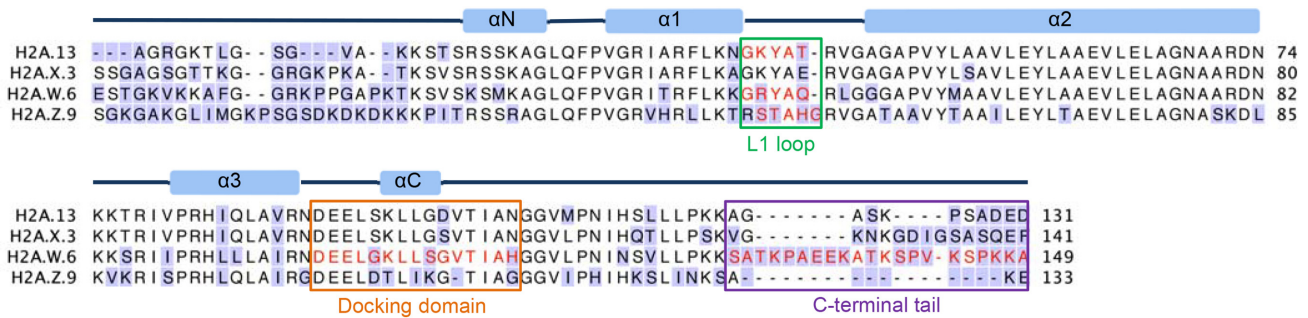
Figure 2. The alignment of *Arabidopsis* histone H2A.13, H2A.X.3, H2A.W.6 and H2A.Z.9. The amino acid residues, which are different compared to another H2A variants, are shown on purple background. The amino acid residues, which were swapped or deleted in this study, are colored in red. The L1 loop, the docking domain and the C-terminal tails are in green, red and purple boxes, respectively.

ure S1B and C. By contrast, H2A-H2B dimers dissociated at slightly higher temperature compared to H2A.W and H2A.X (Figure 3D and Supplementary Figure S1C). Thus, each type of H2A variants confers distinct stability to nucleosomes *in vitro*, with H2A.Z being the most unstable and H2A the most stable.

To investigate the impact of key domains that distinguish H2A.W from H2A.Z (Figure 2), we obtained mutant versions of H2A.W, lacking the C-terminal tail (H2A.W.6ΔCT), or with the L1 loop from H2A.Z (H2A.W.6L1Z), or with both the L1 loop and docking domain from H2A.Z (H2A.W.6L1ddZΔCT) (Figure 3B; see also Figure 4A). We assembled the nucleosomes containing these mutants and analyzed their thermal stability. The deletion of the C-terminal tail of H2A.W (H2A.W.6ΔCT nucleosome) did not affect nucleosome stability (Figure 3E), suggesting that the extended C-terminal tail of H2A.W does not contribute to stability of the H2A.W.6 nucleosome *in vitro*. Furthermore, the nucleosome containing mutant H2A.W with the L1 loop from H2A (H2A.W.6L1A) showed the same stability compared to wild type H2A.W (Supplementary Figure S2). By contrast, nucleosomes containing H2A.W.6L1Z or H2A.W.6L1ddZΔCT displayed increased instability compared with the nucleosome containing wild type H2A.W (Figure 3E and Supplementary Figure S2). These results suggest that both the L1 loop and the docking domain confer a higher stability to nucleosomes containing H2A and H2A.W compared with H2A.Z.

Importance of the L1 loop, the docking domain and the C-terminal tail of H2A.W *in vivo*

To address the function of the L1 loop and the docking domain in H2A.W nucleosomes *in vivo*, we obtained transgenic plants expressing H2A.W with or without the C-terminal tail in combinations with L1 and docking domain replaced by corresponding sequences of H2A.Z (Figure 4A). These constructs were introduced into *h2a.w.6+/- h2a.w.7-/-* plants and T1 plants expressing each transgene in *h2a.w.6-/- h2a.w.7-/-* double mutant were selected to obtain double mutant plants containing one copy of the transgene in T3 generation and expressing each transgene at a level comparable to wild type H2A.W (Supplementary Figure S3).

We performed immunoprecipitation of H2A.W nucleosomes after MNase digestion and found that none of the H2A.W mutants co-precipitated significant amounts of H2A.Z or canonical H2A (Figure 4B). Small amounts of H2A.X were co-precipitated with most H2A.W mutants owing to the low amounts of dinucleosomes in digested chromatin (see also Discussion). Immunostaining of isolated nuclei revealed that all mutant forms of H2A.W localized specifically to pericentric heterochromatin like wild type H2A.W (Supplementary Figure S4). Hence, we concluded that the domains studied do not affect assembly and the heterochromatic location of H2A.W nucleosomes.

Analysis of H3 and H2B co-precipitated with H2A.W revealed that the deletion of the CT decreased levels of co-precipitation of both histones compared to wild type (Figure 4B). Similarly, mutation of each domain decreased the amount of co-precipitated H3 and H2B (Figure 4B). Combinations of mutations of the L1 loop and the docking domain with the deletion of the CT displayed increasing and cumulative effect on nucleosome stability (Figure 4B). The relative stronger impact observed on H2B compared with H3 is likely explained by the fact that the antibody recognizes only three out of a total of eleven H2B variants in *Arabidopsis*. These data suggest that the CT, L1 loop and docking domain of H2A.W have distinct non-overlapping impact on nucleosome stability *in vivo*. Under same experimental conditions we did not observe a comparable instability of H2A.Z nucleosome (Figure 4C), suggesting that the mutations affect directly H2A.W nucleosomes and do not affect H2A.Z nucleosomes in other domains of the chromatin. Altogether our *in vivo* (Figure 4) and *in vitro* (Figure 3) experiments show that the L1 loop, the docking domain and CT of H2A.W and H2A.Z confer distinct properties to nucleosomes but do not affect localization and incorporation into chromatin.

H2A C-terminal tails protect linker DNA

To evaluate the impact of each feature that distinguishes H2A.Z from H2A.W on chromatin accessibility we analyzed the impact of MNase digestion on chromatin from transgenic lines expressing wild type H2A.W.6, H2A.W.6ΔCT, H2A.W.6L1ZΔCT and H2A.W.6L1ddZΔCT. We performed MNase digestion under limiting MNase amounts followed by DNA extrac-

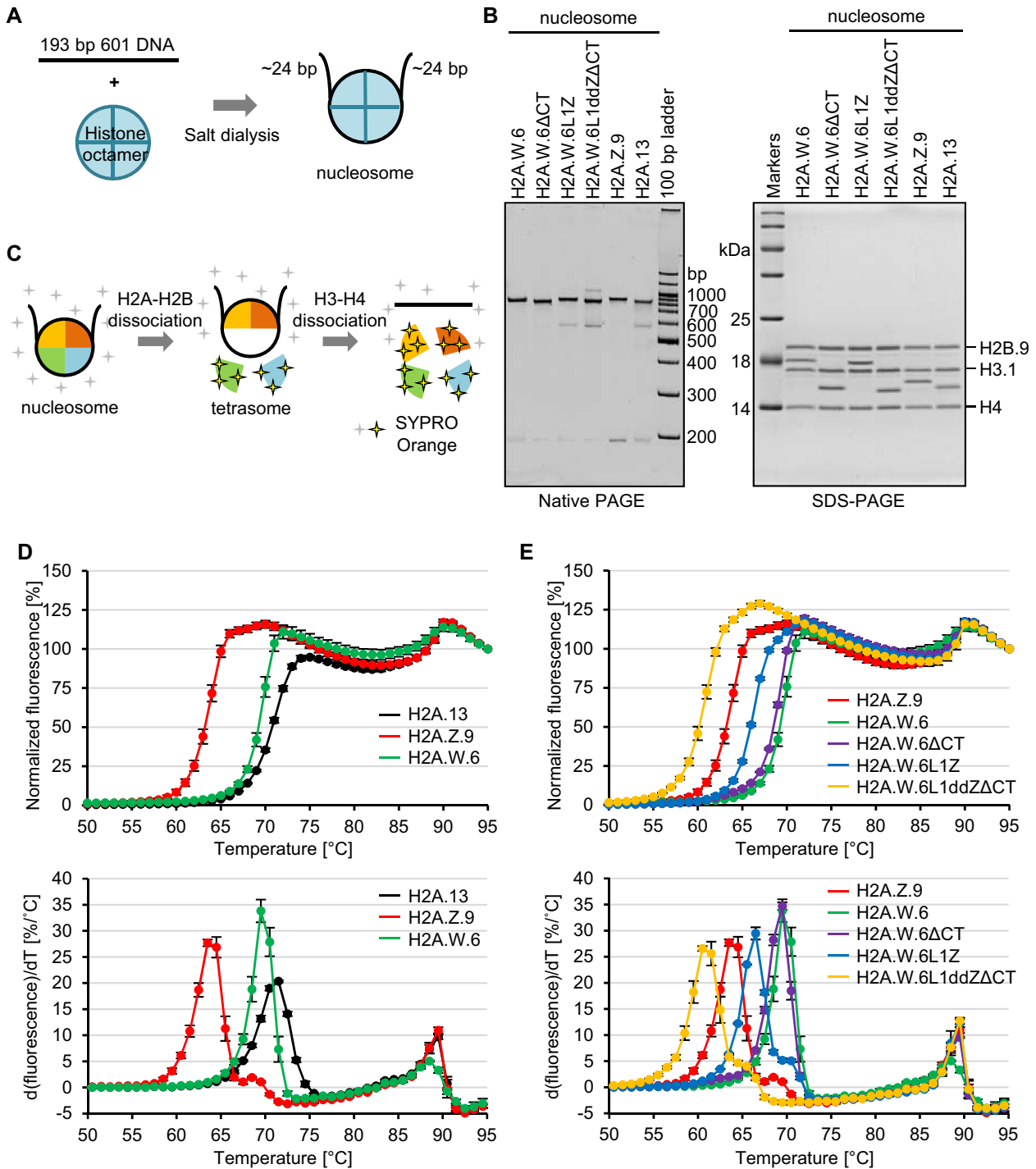**Figure 3.** Thermal stability assay of *Arabidopsis* nucleosomes. (**A**) Schematic presentation of *in vitro* nucleosome reconstitution. All assembled nucleosomes here contain around 24 bp linker DNA. (**B**) Native-PAGE (left) and SDS-PAGE (right) analyses of reconstituted nucleosomes containing H2A.W.6, H2A.W.6ΔCT (lacking the C-terminal tail), H2A.W.6L1Z (W.6 L1 loop replaced by Z.9 sequence), H2A.W.6L1ddZΔCT (W.6 L1 loop and docking domain – dd replaced by Z.9 sequences), H2A.Z.9 and H2A.13 variants. Note slight differences in migration of assembled nucleosomes on native PAGE. (**C**) Schematic presentation of thermal stability assay. SYPRO Orange dye binds only to denatured proteins resulting in fluorescence. (**D** and **E**) Graphical presentation of thermal stability assay of nucleosomes as shown in panel C in the presence of 100 mM NaCl. Normalized values against increasing temperature were plotted from 50°C to 95°C. In lower panel, the derivative values of thermal stability curves shown in upper panel are plotted against each temperature. Presented data are mean of 3 repeats with error bars representing SD. Note that same results were used in D and E for the nucleosomes containing H2A.13, H2A.Z.9 and H2A.W.6. T_m values of the first peak corresponding to H2A–H2B dimer dissociation are 71–72°C (H2A.13 nucleosome), 63–64°C (H2A.Z.9 nucleosome), 69–70°C (H2A.W.6 nucleosome), 69–70°C (H2A.W.6ΔCT nucleosome), 66–67°C (H2A.W.6L1Z nucleosome) and 60–61°C (H2A.W.6L1ddZ ΔCT nucleosome).
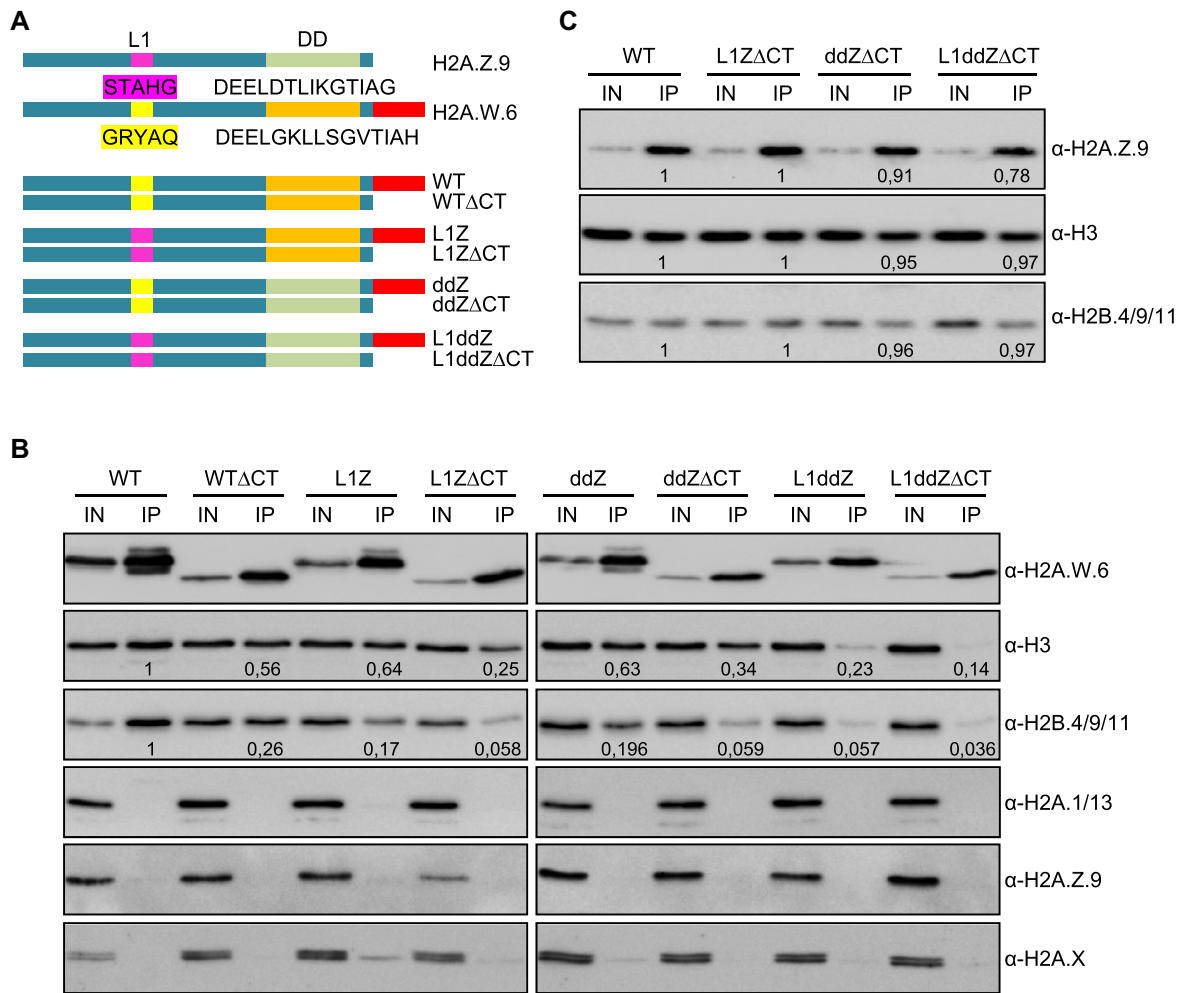
Figure 4. Analysis of H2A.W.6 nucleosomes from transgenic plants expressing H2A.W.6 mutants. (**A**) Schematic presentation of H2A.W.6 mutants in L1 loop and the docking domain. The L1 and docking domain sequences of H2A.W.6 and H2A.Z are also indicated. (**B**) Immunoprecipitation of H2A.W.6 after digestion of nuclei with MNase. Western blotting was performed with antibodies against H2A.W.6, H2A.Z.9, H2A.1/13, H3 and H2B.4/9/11. The numbers below H3 and H2B blots represent their enrichment levels relative to H2A.W.6. The ratios for wild type were set to one and others are expressed relative to wild type. (**C**) Immunoprecipitation of H2A.Z.9 nucleosomes from transgenic plants expressing indicated H2A.W.6 mutants. The numbers below H3 and H2B blots indicate their levels normalized to the enrichment of H2A.Z.9 in each IP, demonstrating that instability of H2A.W.6 mutant nucleosomes is not due to the general effect of the experimental conditions.

tion and profile analysis. We found that deletion of the CT and mutations of L1 and docking domain result in increased accessibility to MNase in a cumulative manner (Figure 5), suggesting that these three regions of H2A might contribute to its role in establishing higher order chromatin structure.

The nucleosome crystal structure suggests that the CT of H2A locates at entry/exit sites of DNA in the nucleosome (41). Furthermore, the impact of the deletion of the CT on nucleosome stability suggested that the extended CT of H2A.W could interact with the linker DNA. To investigate the association of the CT of H2A.W with the linker DNA, we performed the MNase treatment assay on *in vitro* reconstituted nucleosomes containing H2A.W, H2A.WΔCT, H2A and H2A.Z (Figure 6A). In the case of nucleosomes containing H2A and H2A.WΔCT, MNase digestion produced primarily fragments between 140 and 150 bp (Figure 6B, asterisk) corresponding to nucleosome core particle

(Figure 6D). In contrast with H2A or H2A.WΔCT nucleosomes, a more prominent fragment of 155 base-pair or 165 base-pair was detected in H2A.W nucleosome (Figure 6B, C, red arrows, D, E and F), suggesting that the extended C-terminal tail of H2A.W interacts with linker DNA and protects DNA from the cleavage by MNase. Concomitantly, the fragment of 130 bp, which originates from over digestion due to the breathing of DNA ends, was more prominent in H2A or H2A.W.6ΔCT compared to H2A.W nucleosome (Figure 6B and C, blue arrows). Consistent with the presence of a very short C-terminal tail on H2A.Z, the strong 155 bp fragment, resulting from the DNA protection by the C-terminal tail in H2A.W nucleosome, was almost undetectable in assays performed with H2A.Z nucleosome (Figure 6B, C and F). Together, these results strongly suggest that C-terminal tails of H2A variants have distinct capabilities to interact with linker DNA.
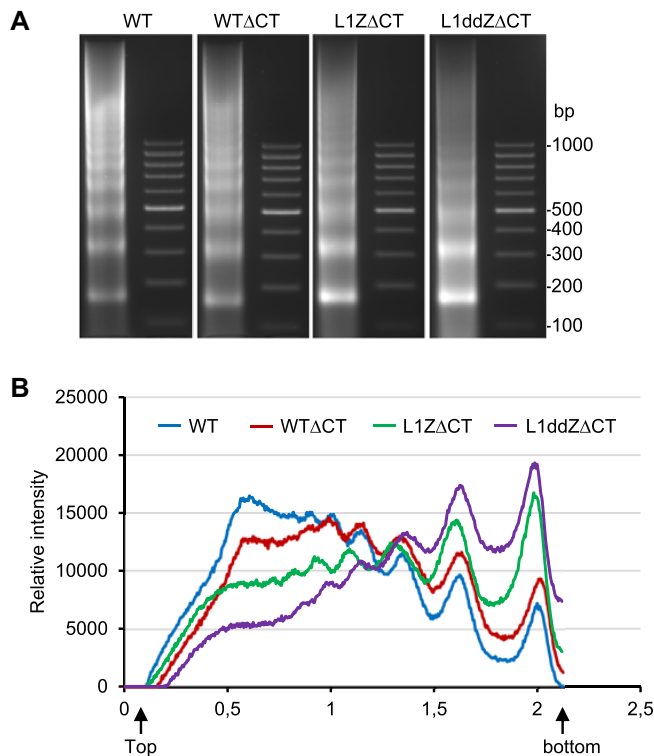
Figure 5. MNase accessibility of chromatin in plants expressing H2A.W.6 mutants. (**A**) Profiles of chromatin from *Arabidopsis* transgenic plants expressing indicated H2A.W.6 mutants. Isolated nuclei were digested for 15 min with 0.1 units of MNase at RT and DNA was extracted and analyzed by 2% agarose gel electrophoresis. (**B**) Quantified profiles of MNase digested nuclei for 15 min.

DISCUSSION

We report here *in vivo* and *in vitro* analyses of nucleosomes containing the four different H2A variants present in *Arabidopsis* chromatin, H2A, H2A.X, H2A.Z and H2A.W. Our data reveals the overwhelming predominance of homotypic nucleosomes in *Arabidopsis* chromatin. Small amounts of H2A and H2A.X co-precipitated with H2A.W nucleosomes most likely reflect the presence of dinucleosomes in MNase digested heterochromatin, which is predominantly occupied by H2A.W but also contains H2A.X and H2A (5,22). However, we can not absolutely exclude the possibility of a small proportion of heterotypic nucleosomes in *Arabidopsis*.

In vitro studies have shown that heterotypic nucleosomes containing H2A and H2A.Z or MacroH2A from animals can assemble (8,13). Homotypic nucleosomes are enriched over active genes in *Drosophila* (42) but heterotypic H2A/H2A.Z nucleosomes are commonly found in *Drosophila*, mice, humans, and budding yeast (38). The predominance of homotypic nucleosomes in *Arabidopsis* implies that plants evolved specific mechanisms responsible for either the assembly/deposition of each type of homotypic nucleosomes or for the removal of heterotypic nucleosomes. Specific mechanisms for the deposition of H2A.Z have been characterized (43) and are conserved in plants (27,44). However, the mechanisms responsible for the establishment of specific genomic profiles of H2A, H2A.X and

H2A.W remain unknown. None of the domains from histones studied here impacts on nucleosome deposition (Supplementary Figure S4), suggesting that each H2A variant carries additional residues or domains responsible for their specific deposition. Based on the strong conservation of key features defining H2A variants in flowering plants (4), it is conceivable that the predominance of homotypic H2A nucleosomes is a general feature of plant chromatin. Similar analysis with chromatin from green algae and non flowering land plants will be required to ascertain this hypothesis from an evolutionary perspective.

There have been controversial reports regarding stability of the H2A.Z nucleosomes in human (18,45), mouse (46) and yeast (47). In agreement with the prediction of specific properties for each type of homotypic nucleosome, we show that H2A, H2A.W, H2A.X and H2A.Z nucleosomes display different properties *in vitro*. Our data demonstrate that H2A.Z confers lower stability compared with other H2A variants as H2A.Z-H2B dissociated from the nucleosome at lower temperature than H2A-H2B (Figure 3). This is consistent with the previous results with human H2A.Z nucleosomes (13). Based on the strong evolutionary conservation of H2A.Z (2), we propose that in eukaryotes nucleosomes homotypic for H2A.Z are less stable than other types of homotypic nucleosomes.

Dissection of conserved domains of H2A variants revealed that the impact of H2A variants on nucleosome stability is primarily due to the L1 and docking domains (6,30,31). Replacement of H2A.W L1 with the corresponding sequence from H2A does not affect nucleosome stability (Supplementary Figure S2). By contrast the L1 loop of H2A.Z decreases stability of H2A.W nucleosome significantly (Figure 3). The modulation of interaction between L1 loops could be influenced by charges carried by specific residues that differentiate this motif among H2A variants and by the flexibility of amino acid side chains (13,18,31). The L1 loops of H2A.W.6 and H2A.13 carry a similar charge (GRYAQ versus GKYAT) in contrast with the L1 loop of H2A.Z (STAHG). In H2A.X and other isoforms of H2A the L1 loop with the sequence GKYAE (except H2A.13 used here; see Supplementary Figure S1A) would carry both positive (on lysine) and negative (on glutamic acid) charge. Thus, the differences we observed are likely due to the change of charge which potentially influence loop–loop and/or loop–DNA interactions and are in line with data from molecular dynamics simulations of the L1 loop from mammalian macroH2A and H2A.Z (48). The docking domain provides interaction surface with H3–H4, and in H2A.W its replacement with the corresponding sequence from H2A.Z further destabilized H2A.W nucleosome (Figure 2). Similarly, deletion of docking domain of H2A or its replacement with the incomplete one from the H2A.Bbd was shown to induce structural changes in the nucleosome (11,49). Thus, weakening interactions between the docking domain and H3 could result in weaker interactions of the H3 αN with DNA at the DNA entry/exit site of the nucleosome. This effect together with the impact of the L1 loop are likely responsible for the faster dissociation of dimers containing H2B and mutant forms of H2A.W from nucleosomes reported in this study.
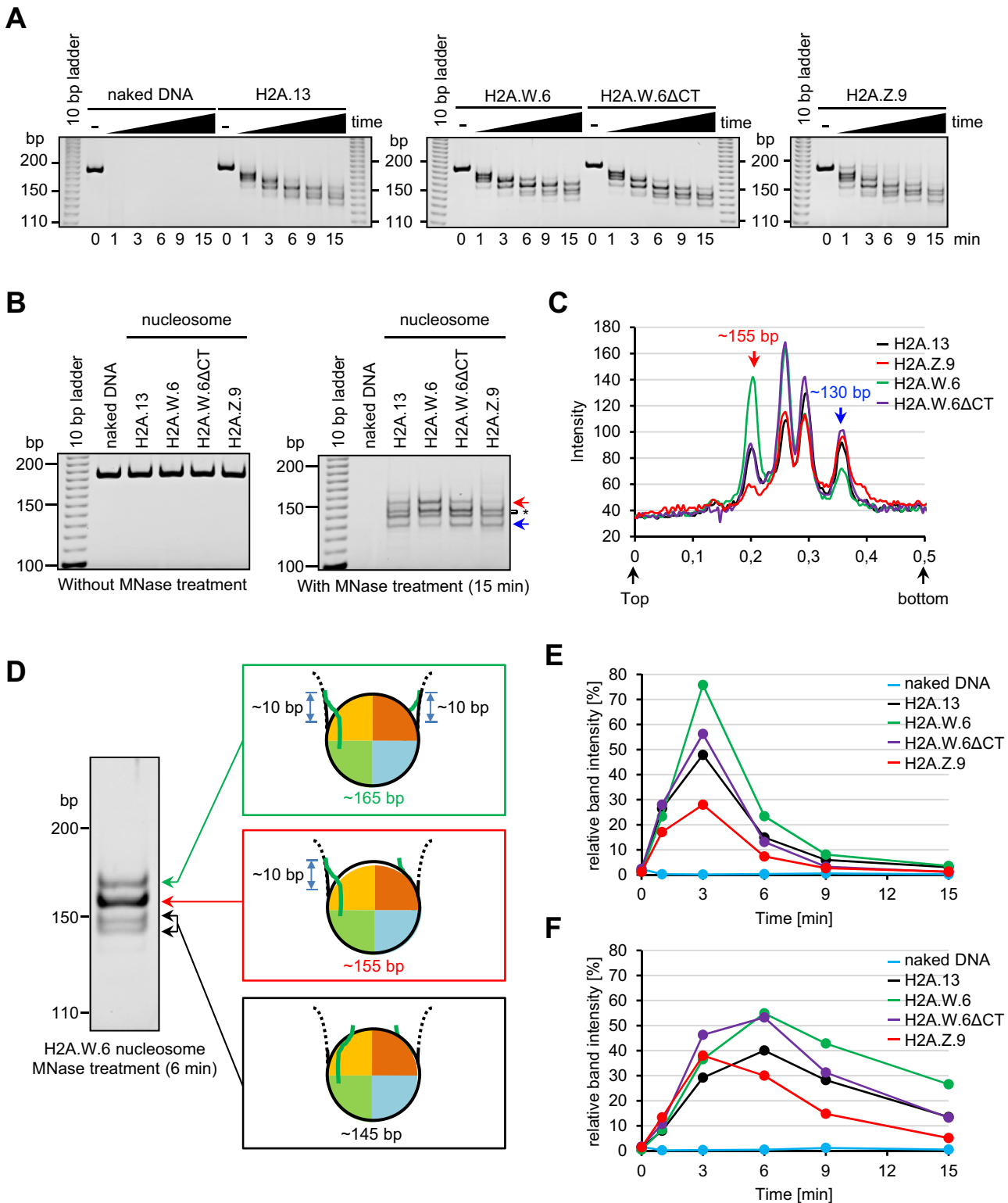
Figure 6. MNase treatment assay. (**A**) *In vitro* assembled nucleosomes containing indicated H2A variants and H2A.W.6 mutants were treated with MNase for indicated times at 25°C and digested DNA was analyzed by native PAGE. (**B**) Native-PAGE analyses of DNA fragments before (left panel) or after 15 min MNase digestion (right panel) of nucleosomes containing indicated H2A variants or H2A.W.6 mutants. The red and blue arrow indicate the top and bottom bands, respectively used for the quantification shown in panel C. (**C**) Graphical presentation of DNA fragments distribution after 15 min digestion with MNase shown in panel B. (**D**) Schematic representation of the 165, 155 or 145 bp fragment obtained by MNase treatment. (**E** and **F**) Graphical representation of the band intensity of ∼165 bp (panel E) or ∼155 bp DNA (panel F) fragments obtained by addition of MNase at indicated times. The intensity of each band was normalized to 193 base-pair DNA fragment corresponding to time point 0 in panel A.

Truncation of the H2A.W CT did not affect nucleosome stability *in vitro* but did affect chromatin accessibility and dissociation of H2A–H2B dimers in additive manner with replacement of the L1 loop and the docking domain by corresponding sequences of H2A.Z. Similarly, in mammals, truncations of H2A CT reduce nucleosome stability *in vivo*, enhance thermal nucleosome mobility *in vitro*, and reduce ability of chromatin remodeler to mobilize nucleosomes *in vitro*, pointing towards the influence of the H2A CT in defining specific and stable nucleosome positions (49,50). These data suggest that the C-terminal tails typical of each type of H2A variant provide distinct functions in chromatin organization.

The CT of H2A.W of *Arabidopsis* limits chromatin accessibility *in vitro*. Similarly in wheat, H2A.W protects more linker DNA (51) and in mammals, the linker domain of macroH2A, which also contains a KSPKK motif, decreases accessibility of extranucleosomal DNA at the entry/exit site of the nucleosome (52). The position of the KSPKK motif at the very C-terminus of H2A.W is compatible with its involvement in contacting the linker DNA. Similarly, molecular dynamics simulations with a nucleosome containing human H2A revealed that its C-terminal tail can protect up to 15 nucleotides of the linker DNA (53,54). We observed similar effect with recombinant *Arabidopsis* H2A nucleosome (Figure 6B, D and F). However the turn-over of 155 bp fragments appeared to be much faster compared to that of H2A.W nucleosome (Figure 6B and F). This difference could be caused by the fact that the CT of H2A.W is ten amino acid residue longer than the CT of H2A, but also by strong differences in charges carried by these two CTs (Figure 2). Two possible scenarios could be envisaged to explain how the CT might influence nucleosome properties and chromatin organization. Depending on the length of the CT, its interaction with the linker DNA together with the H3 N-terminal tail would prevent fluctuations of DNA ends thereby stabilizing the nucleosome (30,31,53–55). As an alternative hypothesis, the CT could impact binding of the linker histone H1 to chromatin. In animals, canonical H2A nucleosomes bind the linker histone more efficiently than H2A.Z (56–58). This interaction depends on the CT (50), suggesting that the longer CT of H2A.W could interact more closely with H1. Based on these and our findings, we propose that H2A variants regulate chromatin accessibility through interaction with linker DNA. In *Arabidopsis*, deletion of the H2A.W affects condensation of constitutive heterochromatin, suggesting that the interaction between CT of H2A variants and linker DNA is relevant *in vivo* (22). The SPKK motif was reported to preferentially bind AT-rich DNA (59), which is a feature of pericentric heterochromatin occupied by H2A.W in *Arabidopsis*. Whether the KSPKK motif interacts with linker DNA directly or this interaction involves H1 or other chromatin associated proteins remains to be determined.

H2A.W was initially characterized by its impact on chromatin higher order structures and this property was confirmed by assays using nucleosomes arrays *in vitro* (22). Here, we further support by *in vivo* data the idea that CT, L1 and the docking domain cooperate to contribute properties specific to the role played by H2A.W in higher order domains of chromatin. How such domains are organized is not understood but might involve two distinct types of mechanisms. Highly positively charged CT from H2A.W might coat certain regions of heterochromatin such as provoking phase separation as proposed in the case of HP1 in *Drosophila* heterochromatin (60,61). Alternatively, specific factors could bind H2A.W CT and bridge nucleosomes arrays into multilayered assemblies of microscopic dimensions.

SUPPLEMENTARY DATA

Supplementary Data are available at NAR Online.

REFERENCES

1. Ray-Gallet,D. and Almouzni,G. (2010) Nucleosome dynamics and histone variants. *Essays Biochem.*, **48**, 75–87.
2. Talbert,P.B., Ahmad,K., Almouzni,G., Ausio,J., Berger,F., Bhalla,P.L., Bonner,W.M., Cande,W.Z., Chadwick,B.P., Chan,S.W. *et al.* (2012) A unified phylogeny-based nomenclature for histone variants. *Epigenet. Chromatin*, **5**, 7.
3. Talbert,P.B. and Henikoff,S. (2017) Histone variants on the move: substrates for chromatin dynamics. *Nat. Rev. Mol. Cell. Biol.*, **18**, 115–126.
4. Kawashima,T., Lorkovic,Z.J., Nishihama,R., Ishizaki,K., Axelsson,E., Yelagandula,R., Kohchi,T. and Berger,F. (2015) Diversification of histone H2A variants during plant evolution. *Trends Plant Sci.*, **20**, 419–425.
5. Lorkovic,Z.J., Park,C., Goiser,M., Jiang,D., Kurzbauer,M.T., Schlogelhofer,P. and Berger,F. (2017) Compartmentalization of DNA damage response between heterochromatin and euchromatin is mediated by distinct H2A histone variants. *Curr. Biol.*, **27**, 1192–1199.
6. Buschbeck,M. and Hake,S.B. (2017) Variants of core histones and their roles in cell fate decisions, development and cancer. *Nat. Rev. Mol. Cell. Biol.*, **18**, 299–314.
7. Zink,L.M. and Hake,S.B. (2016) Histone variants: nuclear function and disease. *Curr. Opin. Genet. Dev.*, **37**, 82–89.
8. Chakravarthy,S., Bao,Y., Roberts,V.A., Tremethick,D. and Luger,K. (2004) Structural characterization of histone H2A variants. *Cold Spring Harb. Symp. Quant. Biol.*, **69**, 227–234.
9. Tachiwana,H., Kagawa,W. and Kurumizaka,H. (2012) Comparison between the CENP-A and histone H3 structures in nucleosomes. *Nucleus*, **3**, 6–11.
10. Taguchi,H., Xie,Y., Horikoshi,N., Maehara,K., Harada,A., Nogami,J., Sato,K., Arimura,Y., Osakabe,A., Kujirai,T. *et al.* (2017) Crystal structure and characterization of novel human histone H3 variants, H3.6, H3.7, and H3.8. *Biochemistry*, **56**, 2184–2196.

11. Arimura,Y., Kimura,H., Oda,T., Sato,K., Osakabe,A., Tachiwana,H., Sato,Y., Kinugasa,Y., Ikura,T., Sugiyama,M. *et al.* (2013) Structural basis of a nucleosome containing histone H2A.B/H2A.Bbd that transiently associates with reorganized chromatin. *Sci. Rep.*, **3**, 3510.

12. Henikoff,S., Thakur,J., Kasinathan,S. and Talbert,P.B. (2017) Remarkable evolutionary plasticity of centromeric chromatin. *Cold Spring Harb. Symp. Quant. Biol.*, 033605.

13. Horikoshi,N., Arimura,Y., Taguchi,H. and Kurumizaka,H. (2016) Crystal structures of heterotypic nucleosomes containing histones H2A.Z and H2A. *Open Biol.*, **6**, 160127.

14. Koyama,M. and Kurumizaka,H. (2018) Structural diversity of the nucleosome. *J. Biochem.*, **163**, 85–95.

15. Tachiwana,H., Kagawa,W., Shiga,T., Osakabe,A., Miya,Y., Saito,K., Hayashi-Takanaka,Y., Oda,T., Sato,M., Park,S.Y. *et al.* (2011) Crystal structure of the human centromeric nucleosome containing CENP-A. *Nature*, **476**, 232–235.

16. Urahama,T., Harada,A., Maehara,K., Horikoshi,N., Sato,K., Sato,Y., Shiraishi,K., Sugino,N., Osakabe,A., Tachiwana,H. *et al.* (2016) Histone H3.5 forms an unstable nucleosome and accumulates around transcription start sites in human testis. *Epigenet. Chromatin*, **9**, 2.

17. Kujirai,T., Horikoshi,N., Sato,K., Maehara,K., Machida,S., Osakabe,A., Kimura,H., Ohkawa,Y. and Kurumizaka,H. (2016) Structure and function of human histone H3.Y nucleosome. *Nucleic Acids Res.*, **44**, 6127–6141.

18. Horikoshi,N., Sato,K., Shimada,K., Arimura,Y., Osakabe,A., Tachiwana,H., Hayashi-Takanaka,Y., Iwasaki,W., Kagawa,W., Harata,M. *et al.* (2013) Structural polymorphism in the L1 loop regions of human H2A.Z.1 and H2A.Z.2. *Acta Crystallogr. D Biol. Crystallogr.*, **69**, 2431–2439.

19. Ueda,J., Harada,A., Urahama,T., Machida,S., Maehara,K., Hada,M., Makino,Y., Nogami,J., Horikoshi,N., Osakabe,A. *et al.* (2017) Testis-Specific histone variant H3t gene is essential for entry into spermatogenesis. *Cell Rep.*, **18**, 593–600.

20. Tachiwana,H., Osakabe,A., Kimura,H. and Kurumizaka,H. (2008) Nucleosome formation with the testis-specific histone H3 variant, H3t, by human nucleosome assembly proteins in vitro. *Nucleic Acids Res.*, **36**, 2208–2218.

21. Borg,M. and Berger,F. (2015) Chromatin remodelling during male gametophyte development. *Plant J.*, **83**, 177–188.

22. Yelagandula,R., Stroud,H., Holec,S., Zhou,K., Feng,S., Zhong,X., Muthurajan,U.M., Nie,X., Kawashima,T., Groth,M. *et al.* (2014) The histone variant H2A.W defines heterochromatin and promotes chromatin condensation in Arabidopsis. *Cell*, **158**, 98–109.

23. Rivera-Casas,C., Gonzalez-Romero,R., Cheema,M.S., Ausio,J. and Eirin-Lopez,J.M. (2016) The characterization of macroH2A beyond vertebrates supports an ancestral origin and conserved role for histone variants in chromatin. *Epigenetics*, **11**, 415–425.

24. Barral,S., Morozumi,Y., Tanaka,H., Montellier,E., Govin,J., de Dieuleveult,M., Charbonnier,G., Coute,Y., Puthier,D., Buchou,T. *et al.* (2017) Histone variant H2A.L.2 guides transition Protein-Dependent protamine assembly in male germ cells. *Mol. Cell*, **66**, 89–101.

25. Molaro,A., Young,J.M. and Malik,H. S. (2018) Evolutionary origins and diversification of testis-specific short histone H2A variants in mammals. *Genome Res.*, **28**, 460–473.

26. Millar,C.B. (2013) Organizing the genome with H2A histone variants. *Biochem. J.*, **449**, 567–579.

27. Dona,M. and Mittelsten Scheid,O. (2015) DNA Damage repair in the context of plant chromatin. *Plant Physiol.*, **168**, 1206–1218.

28. Lorkovic,Z.J. and Berger,F. (2017) Heterochromatin and DNA damage repair: use different histone variants and relax. *Nucleus*, **8**, 583–588.

29. Turinetto,V. and Giachino,C. (2015) Multiple facets of histone variant H2AX: a DNA double-strand-break marker with several biological functions. *Nucleic Acids Res.*, **43**, 2489–2498.

30. Bonisch,C. and Hake,S.B. (2012) Histone H2A variants in nucleosomes and chromatin: more or less stable? *Nucleic Acids Res.*, **40**, 10719–10741.

31. Shaytan,A.K., Landsman,D. and Panchenko,A.R. (2015) Nucleosome adaptability conferred by sequence and structural variations in histone H2A-H2B dimers. *Curr. Opin. Struct. Biol.*, **32**, 48–57.

32. Clough,S.J. and Bent,A.F. (1998) Floral dip: a simplified method for Agrobacterium-mediated transformation of Arabidopsis thaliana. *Plant J.*, **16**, 735–743.

33. Tachiwana,H., Kagawa,W., Osakabe,A., Kawaguchi,K., Shiga,T., Hayashi-Takanaka,Y., Kimura,H. and Kurumizaka,H. (2010) Structural basis of instability of the nucleosome containing a testis-specific histone variant, human H3T. *Proc. Natl. Acad. Sci. U.S.A.*, **107**, 10454–10459.

34. Tanaka,Y., Tawaramoto-Sasanuma,M., Kawaguchi,S., Ohta,T., Yoda,K., Kurumizaka,H. and Yokoyama,S. (2004) Expression and purification of recombinant human histones. *Methods*, **33**, 3–11.

35. Arimura,Y., Tachiwana,H., Oda,T., Sato,M. and Kurumizaka,H. (2012) Structural analysis of the hexasome, lacking one histone H2A/H2B dimer from the conventional nucleosome. *Biochemistry*, **51**, 3302–3309.

36. Lowary,P.T. and Widom,J. (1998) New DNA sequence rules for high affinity binding to histone octamer and sequence-directed nucleosome positioning. *J. Mol. Biol.*, **276**, 19–42.

37. Taguchi,H., Horikoshi,N., Arimura,Y. and Kurumizaka,H. (2014) A method for evaluating nucleosome stability with a protein-binding fluorescent dye. *Methods*, **70**, 119–126.

38. Luk,E., Ranjan,A., Fitzgerald,P.C., Mizuguchi,G., Huang,Y., Wei,D. and Wu,C. (2010) Stepwise histone replacement by SWR1 requires dual activation with histone H2A.Z and canonical nucleosome. *Cell*, **143**, 725–736.

39. Nekrasov,M., Amrichova,J., Parker,B.J., Soboleva,T.A., Jack,C., Williams,R., Huttley,G.A. and Tremethick,D.J. (2012) Histone H2A.Z inheritance during the cell cycle and its impact on promoter organization and dynamics. *Nat. Struct. Mol. Biol.*, **19**, 1076–1083.

40. Viens,A., Mechold,U., Brouillard,F., Gilbert,C., Leclerc,P. and Ogryzko,V. (2006) Analysis of human histone H2AZ deposition in vivo argues against its direct role in epigenetic templating mechanisms. *Mol. Cell. Biol.*, **26**, 5325–5335.

41. Luger,K., Mader,A.W., Richmond,R.K., Sargent,D.F. and Richmond,T.J. (1997) Crystal structure of the nucleosome core particle at 2.8 A resolution. *Nature*, **389**, 251–260.

42. Weber,C.M., Henikoff,J.G. and Henikoff,S. (2010) H2A.Z nucleosomes enriched over active genes are homotypic. *Nat. Struct. Mol. Biol.*, **17**, 1500–1507.

43. Billon,P. and Cote,J. (2013) Precise deposition of histone H2A.Z in chromatin for genome expression and maintenance. *Biochim. Biophys. Acta*, **1819**, 290–302.

44. Jarillo,J.A. and Pineiro,M. (2015) H2A.Z mediates different aspects of chromatin function and modulates flowering responses in Arabidopsis. *Plant J.*, **83**, 96–109.

45. Abbott,D.W., Ivanova,V.S., Wang,X., Bonner,W.M. and Ausio,J. (2001) Characterization of the stability and folding of H2A.Z chromatin particles: implications for transcriptional activation. *J. Biol. Chem.*, **276**, 41945–41949.

46. Park,Y.J., Dyer,P.N., Tremethick,D.J. and Luger,K. (2004) A new fluorescence resonance energy transfer approach demonstrates that the histone variant H2AZ stabilizes the histone octamer within the nucleosome. *J. Biol. Chem.*, **279**, 24274–24282.

47. Watanabe,S., Radman-Livaja,M., Rando,O.J. and Peterson,C.L. (2013) A histone acetylation switch regulates H2A.Z deposition by the SWR-C remodeling enzyme. *Science*, **340**, 195–199.

48. Bowerman,S. and Wereszczynski,J. (2016) Effects of MacroH2A and H2A.Z on nucleosome dynamics as elucidated by molecular dynamics simulations. *Biophys. J.*, **110**, 327–337.

49. Shukla,M.S., Syed,S.H., Goutte-Gattat,D., Richard,J.L., Montel,F., Hamiche,A., Travers,A., Faivre-Moskalenko,C., Bednar,J., Hayes,J.J. *et al.* (2011) The docking domain of histone H2A is required for H1 binding and RSC-mediated nucleosome remodeling. *Nucleic Acids Res.*, **39**, 2559–2570.

50. Vogler,C., Huber,C., Waldmann,T., Ettig,R., Braun,L., Izzo,A., Daujat,S., Chassignet,I., Lopez-Contreras,A.J., Fernandez-Capetillo,O. *et al.* (2010) Histone H2A C-terminus regulates chromatin dynamics, remodeling, and histone H1 binding. *PLoS Genet.*, **6**, e1001234.

51. Lindsey,G.G., Orgeig,S., Thompson,P., Davies,N. and Maeder,D.L. (1991) Extended C-terminal tail of wheat histone H2A interacts with DNA of the "linker" region. *J. Mol. Biol.*, **218**, 805–813.

52. Chakravarthy,S., Patel,A. and Bowman,G.D. (2012) The basic linker of macroH2A stabilizes DNA at the entry/exit site of the nucleosome. *Nucleic Acids Res.*, **40**, 8285–8295.

53. Li,Z. and Kono,H. (2016) Distinct roles of histone H3 and H2A tails in nucleosome stability. *Sci. Rep.*, **6**, 31437.

54. Shaytan,A.K., Armeev,G.A., Goncearenco,A., Zhurkin,V.B., Landsman,D. and Panchenko,A.R. (2016) Coupling between histone conformations and DNA geometry in nucleosomes on a microsecond Timescale: Atomistic insights into nucleosome functions. *J. Mol. Biol.*, **428**, 221–237.

55. Biswas,M., Voltz,K., Smith,J.C. and Langowski,J. (2011) Role of histone tails in structural stability of the nucleosome. *PLoS Comput. Biol.*, **7**, e1002279.

56. Bonner,W.M. and Stedman,J.D. (1979) Histone 1 is proximal to histone 2A and to A24. *Proc. Natl. Acad. Sci. U.S.A.*, **76**, 2190–2194.

57. Boulikas,T., Wiseman,J.M. and Garrard,W.T. (1980) Points of contact between histone H1 and the histone octamer. *Proc. Natl. Acad. Sci. U.S.A.*, **77**, 127–131.

58. Thakar,A., Gupta,P., Ishibashi,T., Finn,R., Silva-Moreno,B., Uchiyama,S., Fukui,K., Tomschik,M., Ausio,J. and Zlatanova,J. (2009) H2A.Z and H3.3 histone variants affect nucleosome structure: biochemical and biophysical studies. *Biochemistry*, **48**, 10852–10857.

59. Churchill,M.E. and Suzuki,M. (1989) 'SPKK' motifs prefer to bind to DNA at A/T-rich sites. *EMBO J.*, **8**, 4189–4195.

60. Larson,A.G., Elnatan,D., Keenen,M.M., Trnka,M.J., Johnston,J.B., Burlingame,A.L., Agard,D.A., Redding,S. and Narlikar,G.J. (2017) Liquid droplet formation by HP1alpha suggests a role for phase separation in heterochromatin. *Nature*, **547**, 236–240.

61. Strom,A.R., Emelyanov,A.V., Mir,M., Fyodorov,D.V., Darzacq,X. and Karpen,G.H. (2017) Phase separation drives heterochromatin domain formation. *Nature*, **547**, 241–245.